Published April 5, 2010

Intraflagellar transport molecules in ciliary and nonciliary cells of the retina

Tina Sedmak and Uwe Wolfrum

Department of Cell and Matrix Biology, Institute of Zoology, Johannes Gutenberg University Mainz, D-55099 Mainz, Germany

The assembly and maintenance of cilia require intraflagellar transport (IFT), a process mediated by molecular motors and IFT particles. Although IFT is a focus of current intense research, the spatial distribution of individual IFT proteins remains elusive. In this study, we analyzed the subcellular localization of IFT proteins in retinal cells by high resolution immunofluorescence and immunoelectron microscopy. We report that IFT proteins are differentially localized in subcompartments of photoreceptor cilia and in defined periciliary target domains for cytoplasmic transport, where they are associated with transport vesicles. IFT20 is not in the IFT core complex in photoreceptor cilia but accompanies Golgi-based sorting and vesicle trafficking of ciliary cargo. Moreover, we identify a nonciliary IFT system containing a subset of IFT proteins in dendrites of retinal neurons. Collectively, we provide evidence to implicate the differential composition of IFT systems in cells with and without primary cilia, thereby supporting new functions for IFT beyond its well-established role in cilia.

Introduction

Intraflagellar transport (IFT) was first described in the flagella of *Chlamydomonas* (Kozminski et al., 1993) and has since been proven to be a conserved process in a variety of motile and nonmotile cilia in eukaryotic organisms (Sloboda, 2005). IFT comprises the bidirectional transport of IFT particles containing ciliary or flagellar cargo along the outer doublet microtubules of the axoneme (Rosenbaum and Witman, 2002). These processes ensure the assembly and the molecular turnover of ciliary components (Qin et al., 2004) but also take part in signaling processes generated in the cilium (Wang et al., 2006). Genetic evidence indicates that kinesin-II family members serve as anterograde transport motors in IFT (Kozminski et al., 1995; Cole et al., 1998; Snow et al., 2004), whereas the cytoplasmic dynein 2/1b mediates IFT in the retrograde direction (Pazour et al., 1998, 1999; Signor et al., 1999a). Biochemical analyses revealed that IFT particles are composed of IFT proteins organized into two complexes, A and B (Cole et al., 1998; Cole, 2003). The sequences of IFT proteins are highly conserved between species, and mutations in these genes disturb ciliary assembly in all organisms tested (Cole et al., 1998; Murcia et al., 2000; Pazour et al., 2002; Tsujikawa and Malicki, 2004; Krock and Perkins, 2008; Omori et al., 2008). Nevertheless, the specific functions of the individual IFT proteins in IFT as well as their subcellular and subcompartmental localization in cilia remain to be elucidated (Sloboda, 2005). Interestingly, there is growing evidence for a role of IFT proteins in processes not associated with cilia (Pazour et al., 2002; Follit et al., 2006; Jékely and Arendt, 2006; Finetti et al., 2009; Baldari and Rosenbaum, 2010).

Over the last decade, IFT has been studied intensively in sensory cilia, including photoreceptor cell outer segments (OSs) in the vertebrate retina (e.g., Beech et al., 1996; Pazour et al., 2002; Baker et al., 2003; Insinna et al., 2008, 2009; Krock and Perkins, 2008; Luby-Phelps et al., 2008). Vertebrate photoreceptors are highly polarized sensory neurons consisting of morphologically and functionally distinct cellular compartments. A short axon projects from the cell body of the photoreceptor to form synaptic contact with secondary retinal neurons (bipolar and horizontal cells), and at the opposite pole, a short dendrite is differentiated into the inner segment (IS) and the light-sensitive OS (Fig. 1; Besharse and Horst, 1990; Roepman and Wolfrum, 2007). The OS is similar to other sensory cilia (Insinna and Besharse, 2008) but, in addition, contains specialized

Correspondence to Uwe Wolfrum: wolfrum@uni-mainz.de

Abbreviations used in this paper: BB, basal body; CC, connecting cilium; GA, Golgi apparatus; IFT, intraflagellar transport; INL, inner nuclear layer; IS, inner segment; ONL, outer nuclear layer; OPL, outer plexiform layer; OS, outer segment; RPE, retinal pigment epithelium.

Supplemental Material can be found at:
http://jcb.rupress.org/content/suppl/2010/04/05/jcb.200911095.DC1.html

The Rockefeller University Press $30.00
J. Cell Biol. Vol. 189 No. 1 171–186
www.jcb.org/cgi/doi/10.1083/jcb.200911095

Published April 5, 2010

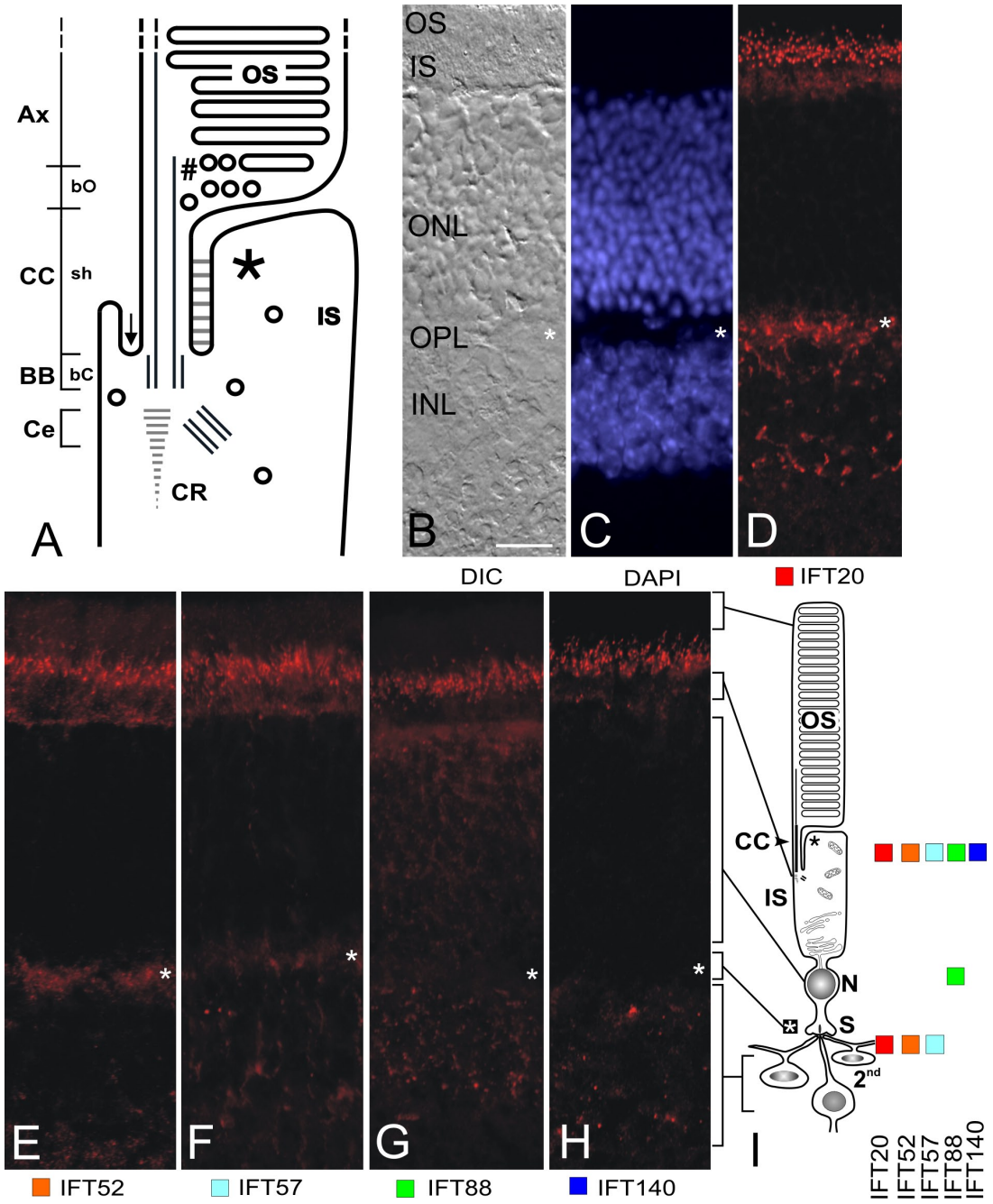

Figure 1. **Localization of IFT proteins in the retina.** (A) Schema of the ciliary apparatus of a rod photoreceptor cell: the photosensitive OS linked by the CC to the IS. The CC is composed of a basal part (bC), which represents the region of the BB, and the CC shaft (sh). The shaft continues into the base of the OS (bO; number sign). Microtubules of the axoneme (Ax) extend into the OS. A centriole (Ce) is adjacent to the BB and the ciliary rootlet (CR). A black asterisk indicates the apical periciliary extension of the IS. The arrow points into the groove between the IS and CC. (B–D) Longitudinal cryosection through a mouse retina. Differential interference contrast (DIC) image (B), DAPI staining (C), and indirect immunofluorescence of anti-IFT20 (D) are shown. (E–H) Immunofluorescence of longitudinal cryosections through mouse retinas stained for IFT52 (E), -57 (F), -88 (G), and -140 (H). (I) Schema of a rod cell and connection to secondary retinal neurons (2nd) illustrating the differential localization of IFT proteins. Photoreceptor cell bodies harboring nuclei (N) are located in the ONL. Synapses (S) to secondary neurons in the OPL (white asterisks) are shown. Bar, 10 µm.

flattened disk-like membranes, where all components of the visual transduction cascade are arranged (Yau and Hardie, 2009). These phototransductive membranes are continually renewed throughout lifetime; newly synthesized membranes are added at the base of the OS, whereas aged disks at the apex are phagocytosed by cells of the retinal pigment epithelium (RPE; Young, 1976). This high membrane turnover implies an efficient and massive vectorial transport of all OS components from the site of their biogenesis in the photoreceptor IS to the base of the OS, the site of disk neogenesis. On its route to the OS, cargo has to be reloaded from IS transport carriers to ciliary transport systems in a specialized compartment of the apical IS (Papermaster, 2002; Roepman and Wolfrum, 2007; Maerker et al., 2008). In addition to the unidirectional constitutive translocations of OS

Published April 5, 2010

molecules, light-dependent bidirectional movement of molecules across the connecting cilium (CC) contributes to the long range light adaptation of rod photoreceptor cells (Calvert et al., 2006). Structural and molecular characteristics qualify the CC as the equivalent of the transition zone localized between the basal body (BB) and the axoneme in proteotypic cilia (Fig. 1 A; Besharse and Horst, 1990; Roepman and Wolfrum, 2007; Insinna and Besharse, 2008). Some microtubules of the CC extend throughout almost the entire length of the OS, where they mediate protein trafficking within the OS (Liu et al., 2002; Reidel et al., 2008).

IFT has been proposed as an essential transport mechanism in photoreceptor cells (Rosenbaum et al., 1999), and its critical importance has been demonstrated subsequently (Pazour et al., 2002; Tsujikawa and Malicki, 2004; Krock and Perkins, 2008). As in other ciliated and flagellated cells, the mode of the IFT operation and the assignment of specific functions to individual IFT proteins are still lacking in photoreceptor cells (Baker et al., 2004; Hou et al., 2007; Bhowmick et al., 2009). A systematic analysis of the subcellular distribution of IFT proteins in photoreceptor cells will provide important insights into the roles of IFT proteins unique for specialized photoreceptor cilia but also into more general processes associated with IFT proteins common to all cilia and flagella. So far, studies on the distribution of IFT proteins in photoreceptor cells were limited to a few immunofluorescence analyses (Pazour et al., 2002; Tsujikawa and Malicki, 2004; Krock and Perkins, 2008) and to a preliminary electron microscopic study on IFT88 (Luby-Phelps et al., 2008), which collectively provided only limited insight into the spatial distribution of IFT proteins.

In this study, we used a combination of high resolution immunofluorescence and immunoelectron microscopy for the analyses of the spatial distribution of IFT proteins in retinal neurons. Our data reveal that IFT proteins are differentially localized in subciliary compartments but also present in nonciliary compartments of photoreceptor cells. Furthermore, the localization of IFT proteins in dendritic processes of nonciliated neurons indicates that IFT protein complexes operate in nonciliated cells and may participate in intracellular vesicle trafficking in eukaryotic cells in general.

Results

Although substantial biochemical and genetic efforts have been undertaken and genetic evidence indicates important roles of each IFT particle protein in the development and maintenance of cilia, the functions of the individual IFT molecules remained largely elusive (Sloboda, 2005). This is partly because of the insufficient knowledge concerning the subcellular localization of the IFT proteins. In this study, we have systematically analyzed the expression and subcellular localization of four different IFT complex B proteins, IFT20, -52, -57, and -88, as well as the complex A protein IFT140 in the mouse retina.

Expression of IFT proteins in the mammalian retina

IFT protein expression was accessed by Western blots using previously characterized affinity-purified polyclonal antibodies raised to murine IFT proteins (Pazour et al., 2002; Baker et al., 2003; Follit et al., 2006). These experiments verified the expression of all five IFT proteins in the murine retina (Fig. S1, A and B). The antibodies to four IFT proteins each recognized a single band of expected size in retinal protein extracts, which implied that these antibodies are monospecific. Only anti-IFT52 detected a second band with a slightly lower molecular weight in retinal extracts, which was not observed in analyses of testis samples (Fig. S1, A and C). This band might be caused by a splice variant of IFT52, which is expressed in the retina but is absent in testis.

The retina is composed of well-defined layers consisting of specific cell types or even at subcellular compartments of retinal cells (Fig. 1). This spatial organization makes it relatively easy to determine the subcellular localization of proteins in retinal sections, even under light microscopy. To determine the subcellular distribution of IFT proteins in the retina, cryosections of mouse eye were analyzed by indirect immunofluorescence. As expected from previous studies (Pazour et al., 2002; Krock and Perkins, 2008), all IFT molecules were most abundant in the photoreceptor layer of the retina (Fig. 1). Weak immunoreactivity for IFT88 was also found in the outer nuclear layer (ONL), where the perikarya of the photoreceptor cells are located (Fig. 1 G), and for all IFT molecules in the inner nuclear layer (INL), where the perikarya of the secondary retinal neurons are found (Fig. 1, D–H). Immunostaining for IFT20, -52, and -57 was also observed in the outer plexiform layer (OPL), which contains the presynaptic terminals of photoreceptor cells connected to the postsynaptic terminals of the dendritic processes in secondary retinal neurons, namely bipolar and horizontal cells (Fig. 1, D–F). In addition, IFT20 was expressed in the cells of the RPE and in the ganglion cell layer (Fig. S2 A). The localization of these five IFT proteins in the mouse retina (Fig. 1 I) was identical to that found by indirect immunofluorescence in human and bovine retinas (Fig. S3). To exclude epitope masking by fixation (Follit et al., 2006), we also performed immunocytochemistry on methanol-fixed cryosections and observed no changes in immunostaining (Fig. S4).

Differential subciliary localization of IFT proteins in the photoreceptor cilium

To elucidate the subciliary localization of IFT proteins in the photoreceptor cell layer of the mouse retina, cryosections were analyzed by double labeling with antibodies against IFT proteins and markers of subciliary compartments. Double labeling with anti–centrin-3, a marker for the CC, the BB, and the adjacent centriole (Trojan et al., 2008), and with antibodies to IFT proteins allowed us to determine the spatial localization of IFT proteins in the photoreceptor ciliary apparatus (Fig. 2).

High resolution immunofluorescence imaging of double labeled specimens revealed different subciliary localization of the IFT proteins, as shown in Fig. 2. Double labeling experiments revealed that IFT52, -57, -88, and -140 were concentrated on the tip of the CC in the OS base (Fig. 2, B′–E′). IFT88 and -140 were also detected in the axoneme, which extended further into the distal part of the OS of photoreceptors (Fig. 2, D′ and E′). Latter axonemal localization of these IFT proteins was confirmed

Published April 5, 2010

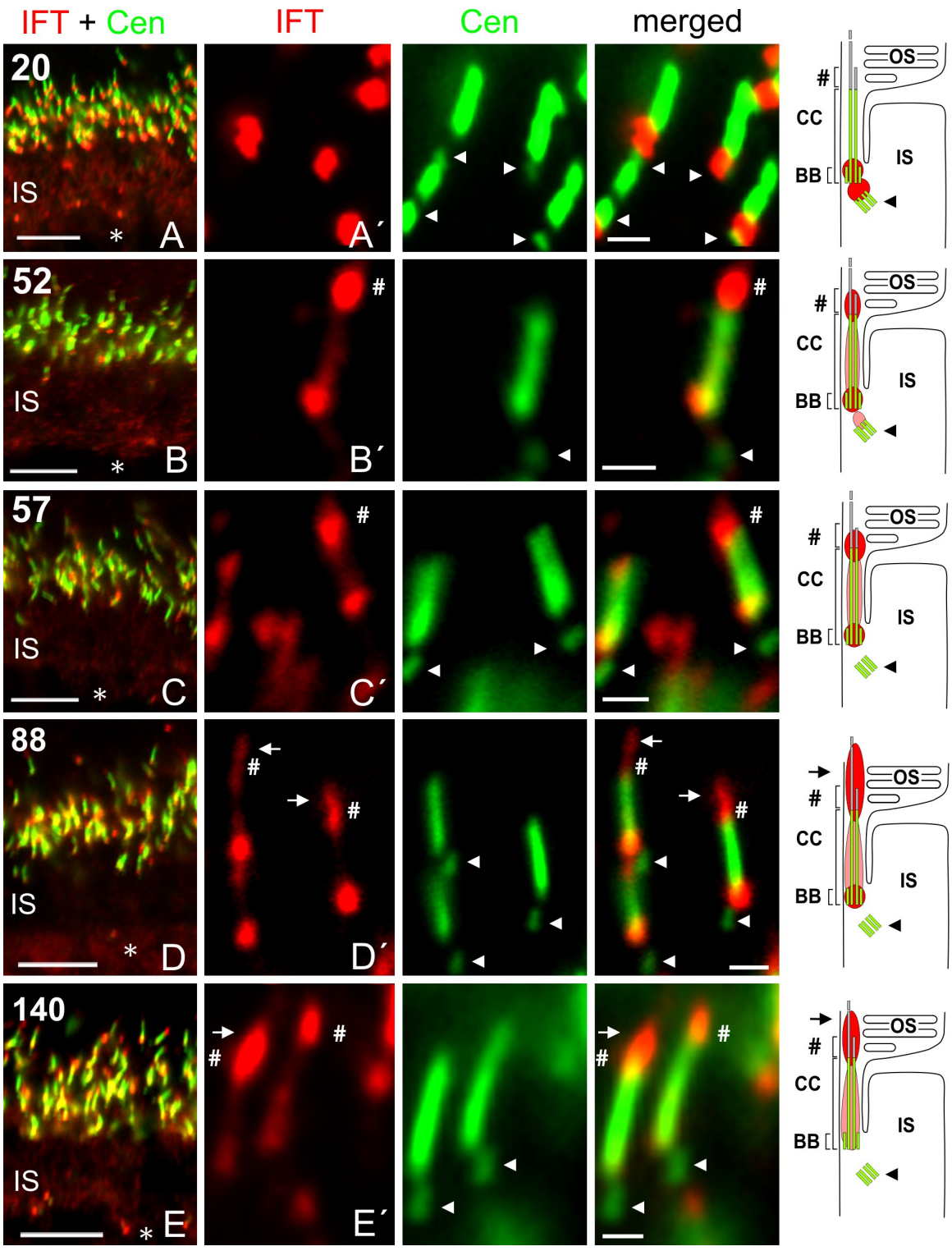

Figure 2. **Differential localization of IFT proteins in photoreceptor cell cilia.** (A–E) Merged images of indirect immunofluorescence double labeling with antibodies to IFT proteins and the ciliary marker anti–centrin-3 (Cen) in cryosections through mouse retinas. (A′–E′) High magnification images of double immunofluorescences in ciliary parts of photoreceptor cells and schemes illustrating subciliary localizations of IFT proteins in relation to centrin-3 located in the CC, its ciliary shaft, its BB, and at the adjacent centriole (arrowheads). IFT20 is present in the basal part of the CC and at the centriole, where IFT52 is also found. IFT52, -57, -88, and -140 are located in the CC, concentrated in its basal part and the OS base (number signs); IFT88 and -140 staining further extends into the axoneme (arrows) of the OS. Asterisks indicate nuclei. Bars: (A–E) 5 µm; (A′–C′ and E′) 0.5 µm; (D′) 1 µm.

by double labeling with an antibody to RP1, a molecular marker for the photoreceptor axoneme (Fig. S2 C; Liu et al., 2002). Weaker staining of IFT52, -57, -88, and -140 was present along the shaft of the CC (Fig. 2, B′–E′). Strong immunoreactivity for IFT52, -57, and -88 was also observed in the basal part of the CC, whereas the anti-IFT140 immunofluorescence was less

Published April 5, 2010

intense in this area (Fig. 2, B′–E′). In contrast to the other IFT proteins analyzed, IFT20 was only detected in the basal part of the CC and at the distal region of the adjacent centriole (Fig. 2 A′). We also detected weak immunofluorescence of IFT52 at the centriole (Fig. 2 B′).

To pinpoint the subcellular localization of the IFT molecules in photoreceptor cells more precisely, we performed immunoelectron microscopy, accessing our recently introduced preembedding labeling technique (Maerker et al., 2008; Sedmak et al., 2009). Our electron microscopy data confirmed the subciliary localization of the IFT proteins in photoreceptor cells, as demonstrated by immunofluorescence. Furthermore, they provided deeper insights into the spatial distribution of IFT proteins in retinal cells. Exploiting the high resolution of the electron microscope, we observed IFT52, -57, -88, and -140 labeling in the OS base and in the basal part of the photoreceptor CC (Fig. 3, A and E; Fig. 4, A and D; and Fig. 5, A and D). In addition, IFT57, -88, and -140 were routinely detected alongside the microtubule doublets in the shaft of the CC (Fig. 3, D and G; and Fig. 4, A and D), whereas IFT52 was concentrated in patches associated with the ciliary membrane and microtubule doublets (Fig. 5 A). The IFT88 and -140 staining extended along the axoneme further into the photoreceptor OS (Figs. 3 E and 4 A). The intense labeling of IFT88 at the axoneme of the OS (Fig. 3 H) is consistent with recently published data on GFP-tagged IFT88 in transgenic frogs (Luby-Phelps et al., 2008). At the base of the CC, IFT52, -57, -88, and -140 were consistently associated with the BB (Fig. 3, A, E, and I; Fig. 4, A and C; and Fig. 5 D). In addition, IFT57, -88, and -140 were regularly concentrated beneath the periciliary groove (Fig. 3, A, E, and I; and Fig. 4 A), in the region where the IFT particle assembly has been suggested in *Chlamydomonas* (Deane et al., 2001). Furthermore, clusters of immunolabeling by antibodies to IFT57, -88, and -140 were routinely observed at vesicle-like structures in the periphery of the basal bodies and of the adjacent centriole in the cytoplasm of the photoreceptor IS (Fig. 3, A, C, and I; and Fig. 4 C). To emphasize vesicles and vesicle-like structures hardly recognizable in the low contrast images of the present immunoelectron microscopy analysis, we provide images at higher magnification of selected regions with and without colorized vesicles (Fig. 3, C, C′, I, and I′; and Fig. 4, C and C′). These results are consistent with the idea that IFT proteins are associated with IFT protein complexes and vesicles in the region surrounding the BB–centriole complex of the photoreceptor cell (Luby-Phelps et al., 2008).

Immunoelectron microscopy further revealed that the immunofluorescence labeling of IFT20 in the basal part of the CC represents the BB of the photoreceptor CC (Fig. 6 A). Similar to the other IFT proteins investigated, the immunoelectron microscopy staining of IFT20 and -52 also appeared in clusters in the cytoplasm at the periphery of the BB and the adjacent centriole of the CC (Fig. 6 A). In contrast to the group of IFT57, -88, and -140, IFT20 and -52 were absent from the ciliary groove (Figs. 5 and 6 A). However, substantial immunoelectron microscopic labeling of IFT20 and -52 was found in the cytoplasm of the periciliary collar-like extension of the photoreceptor IS (Fig. 5, A and C; and Fig. 6, A and C). In this periciliary specialization,

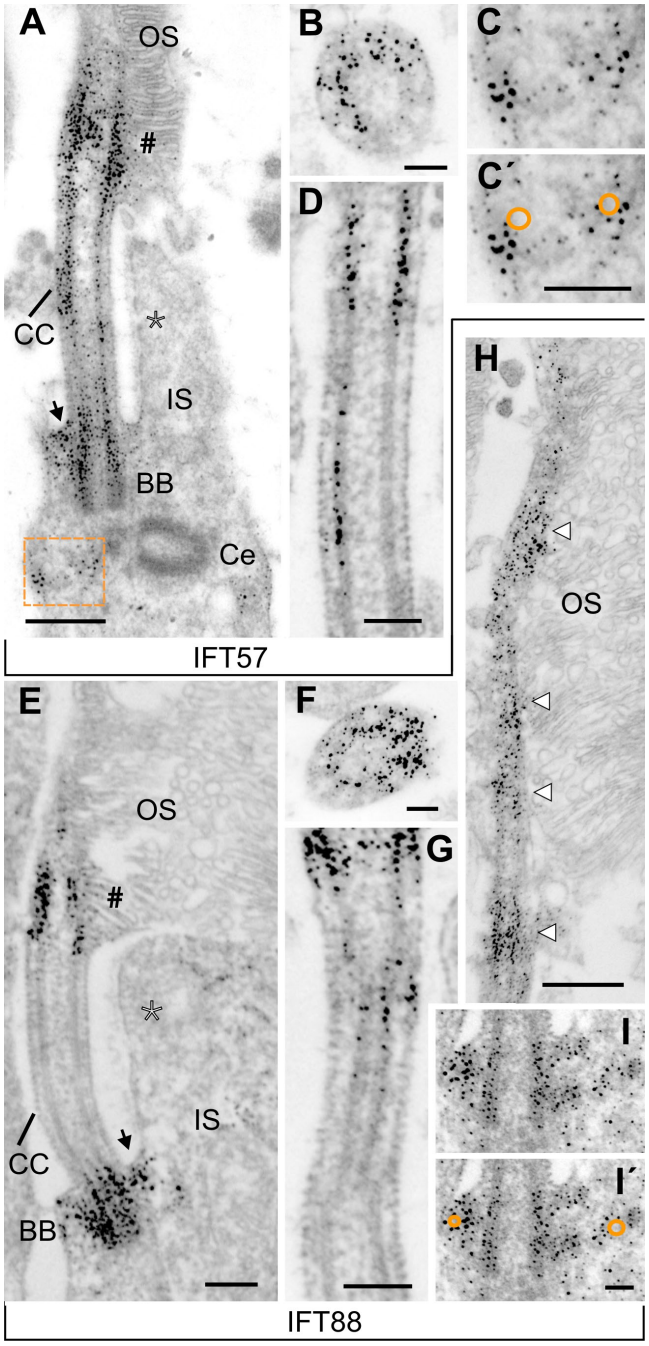

Figure 3. **Immunoelectron microscopic localization of IFT57 and -88 in mouse photoreceptor cells.** (A–I) Electron micrographs of anti-IFT57 (A–D) and -IFT88 (E–I) immunolabeling in sections through parts of mouse photoreceptor cells. (A and E) Longitudinal section through the photoreceptor ciliary apparatus. Cross section (B and F) and longitudinal section (D and G) through the shaft of the CC. (H) Longitudinal section through the axoneme (arrowheads) extending into the OS. IFT57 is concentrated at the OS base (number signs) and in the BB region of the CC but also along microtubules in the CC shaft. In the IS, IFT57 is located below the ciliary groove (arrow) but neither at the centriole (Ce) nor in the periciliary extension of the apical IS (asterisk; A–D). IFT88 is concentrated at the OS base (number signs) and in the BB of the CC, whereas the CC shaft is sparsely stained. In the IS, IFT88 is located below the ciliary groove (arrow) but not in the periciliary apical IS extension (asterisk). (C) Higher magnification image of A (orange rectangle); IFT57 association with vesicle-like structures is highlighted by orange circles in C′. (I) Higher magnification of IFT88 association with vesicle-like structures in the periphery of the BB in the IS, highlighted by orange circles in I′. Bars: (A and H) 0.4 µm; (B, F, I, and I′) 0.1 µm; (C–D, and G) 0.2 µm; (E) 0.25 µm.

Published April 5, 2010

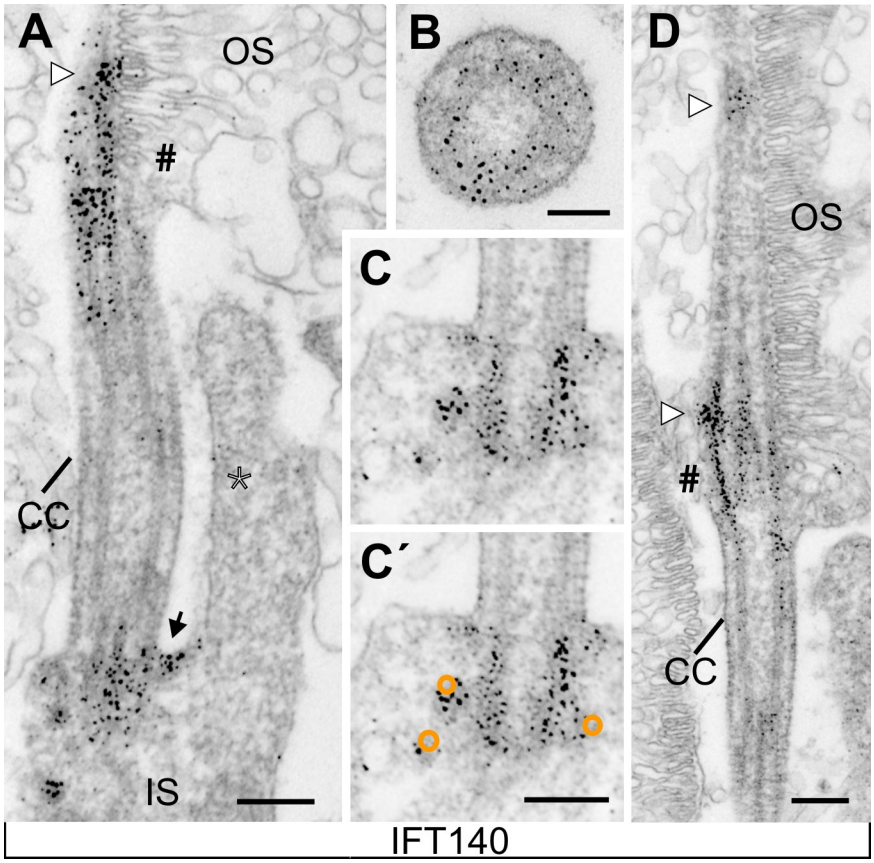

Figure 4. **Immunoelectron microscopic localization of IFT140 in parts of mouse photoreceptor cells.** (A and D) Electron micrographs of anti-IFT140 immunolabeling in longitudinal sections through photoreceptor ciliary apparatus. (B) Cross section through the apical CC. Anti-IFT140 labeling is detected mainly in the OS base (number signs) and at the BB. IFT140 is additionally present in the axoneme (arrowheads) projecting into the OS and in the IS below the ciliary groove (arrow) but not at the periciliary apical IS extension (asterisk). (C) In the periphery of the BB, IFT140 is associated with vesicle-like structures, highlighted by orange circles in C′. Bars: (A and C–D) 0.2 µm; (B) 0.1 µm.

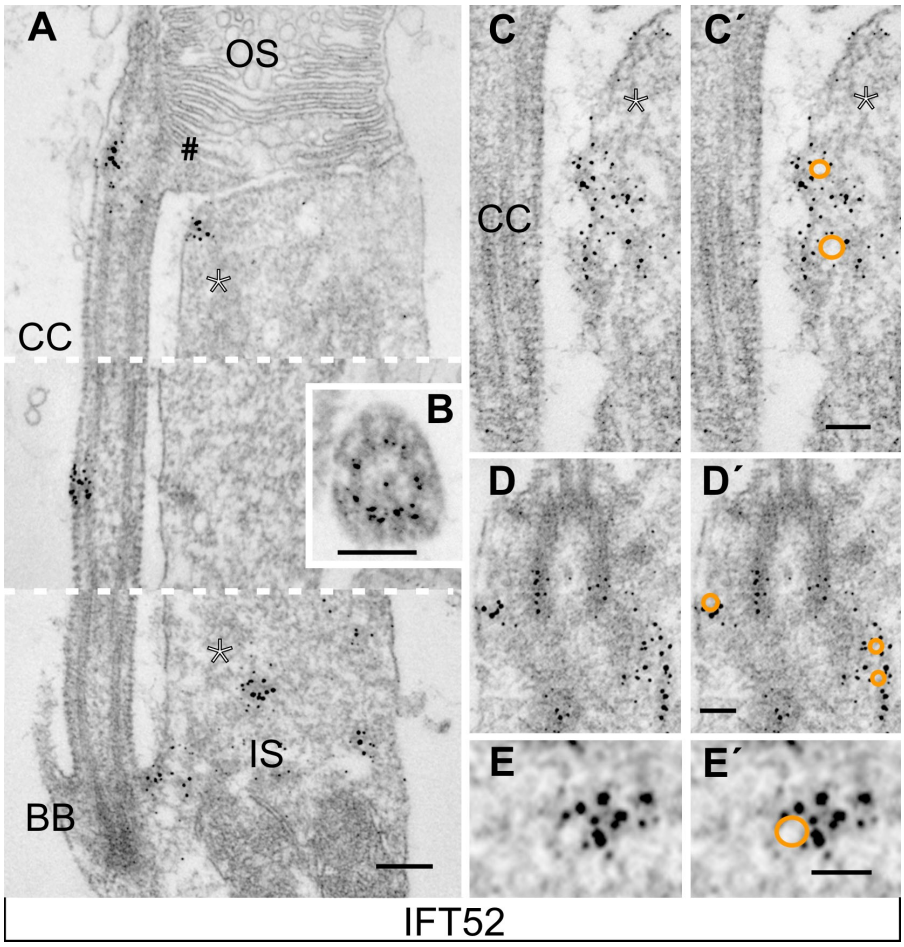

Figure 5. **Immunoelectron microscopic localization of IFT52 in mouse photoreceptor cells.** (A–E) Electron micrographs of anti-IFT52 immunolabeling in sections through parts of mouse photoreceptor cells. (A) Longitudinal sections through the ciliary region (images from three different photoreceptor cells). (B) Cross section through the shaft of the CC. IFT52 immunolabeling is present at the OS base (number sign), in a particle-like structure in the shaft of the CC, and in the periciliary apical IS extension (asterisks). (C) Longitudinal section through periciliary apical IS extension (asterisks). IFT52 is labeled at vesicle-like structures, highlighted by orange circles in C′. (D) IFT52 labeling in a longitudinal section through the BB region. IFT52 is decorated at a vesicle-like structure in the periphery of the BB, highlighted by orange circles in D′. (E) Higher magnification IFT52 labeling clustered at a vesicle-like structure in the IS, highlighted by the orange circle in E′. Bars: (A) 0.4 µm; (B) 0.25 µm; (C–E′) 0.1 µm.

Published April 5, 2010

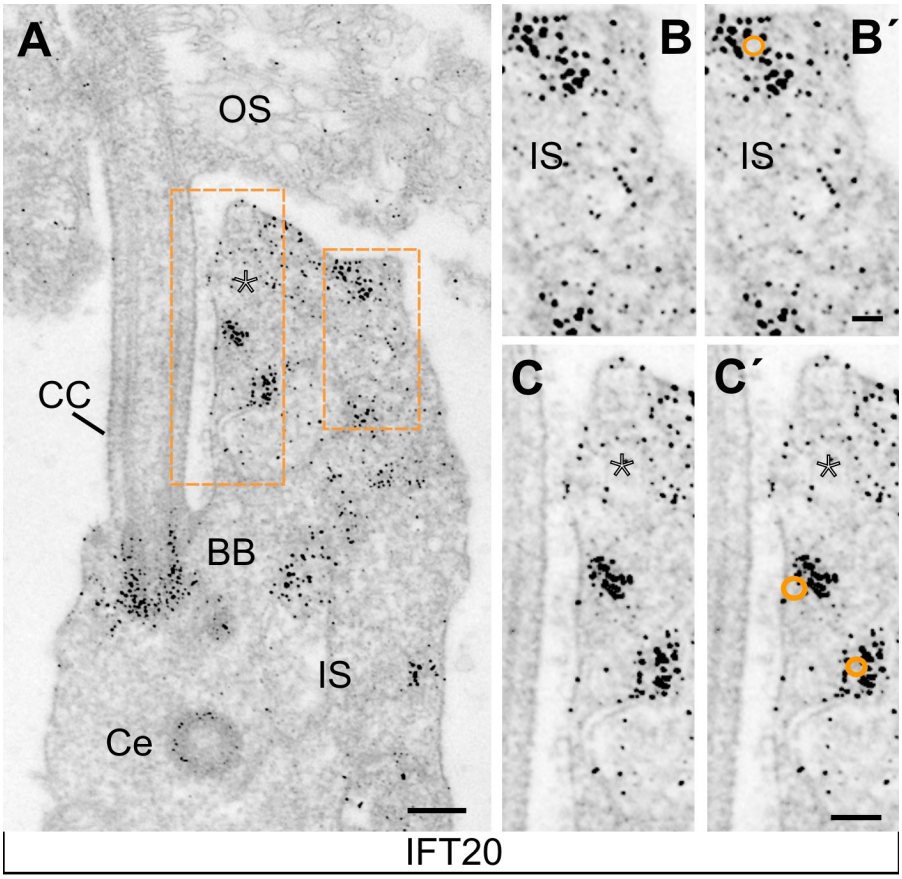

Figure 6. **Immunoelectron microscopic localization of IFT20 in mouse photoreceptor cells.** (A–C) Electron micrographs of anti-IFT20 immunolabeling in longitudinal sections through parts of mouse photoreceptor cells. (A) Anti-IFT20 immunolabeling in the photoreceptor ciliary apparatus. IFT20 is decorated at the BB but not in other parts of the CC or at the OS base. In the IS, IFT20 is located at the apical region of the centriole (Ce) and in the cytoplasm of the periciliary apical IS extension (asterisk). (B and C) Higher magnification of parts of the periciliary IS extension of A (orange rectangles) showing the association of IFT20 with vesicle-like structures, highlighted by orange circles in B′ and C′. Bars: (A) 0.2 µm; (B and B′) 0.05 µm; (C and C′) 0.1 µm.

IFT20 and -52 were concentrated in clusters at vesicle-like structures in the cytoplasm and affiliated with the membrane of the IS facing the membrane of the CC (Fig. 5, A and C; and Fig. 6, B and C). The latter periciliary membrane domain of the apical IS has been recently identified as a target for docking and fusion of cargo vesicles transported through the IS on their destination to the OS (Liu et al., 2007; Maerker et al., 2008), suggesting the involvement of IFT20 and -52 in these processes.

Association of IFT proteins with the Golgi apparatus (GA) and post-Golgi transport vesicles

Inspired by our aforementioned results, we next explored the subcellular distribution of IFT proteins in the Golgi regions of retinal neurons. We performed double labeling with antibodies against IFT20 and the Golgi resident GM130 (Nakamura et al., 1995), which was previously introduced as a reliable Golgi marker in photoreceptor cells (Mazelova et al., 2009). These analyses revealed a partial colocalization of IFT20 with GM130 in the IS of photoreceptor cells (Fig. 7, A and A′) and the cell bodies of the secondary retinal neurons (bipolar and horizontal cells) in the INL (Fig. 7, E–G′). In addition, we found a colocalization of IFT20 with GM130 in ganglion cells and in the nonneuronal cells of the RPE (Fig. S2 A). Immunoelectron microscopy analysis of photoreceptor cells confirmed that IFT20 is associated with the membrane stacks of the GA and vesicle-like structures, which most probably represent post-Golgi transport vesicles (Fig. 7, B–D′; Sung and Tai, 2000; Maerker et al., 2008). Additionally, immunoelectron microscopy analysis confirmed IFT20 labeling of the GA in secondary retinal neurons (Fig. 7, F–G′). In contrast to IFT20, IFT52, -57, -88, and -140 were not detected in the Golgi of retinal cells.

Localization of IFT proteins in dendritic processes of nonciliated retinal neurons

The present immunofluorescence results as well as a previous study in mammalian retinas have indicated expression of IFT proteins in the OPL of the retina (Pazour et al., 2002), which contains the synapses between the photoreceptor cells and dendritic processes of secondary retinal neurons. Our present immunofluorescence data confirm the presence of IFT20, -52, and -57 but not of IFT88 and -140 in the OPL (Fig. 1 and Fig. S2 B). The precise localization of IFT proteins in the synaptic region was assessed by another series of double labeling experiments in which antibodies to the IFT proteins were colabeled with synaptic markers. Costaining of IFT proteins with antibodies against RIBEYE, a specific marker of the photoreceptor ribbon synapse (tom Dieck et al., 2005), did not show any overlap in the resulting immunofluorescence (Fig. 8, A–C). IFT20, -52, and -57 were localized below the ribbon synapse labeling of RIBEYE, indicating the presence of these IFT proteins in the postsynaptic terminals and dendritic processes of bipolar and horizontal cells. Preembedding immunoelectron microscopy analysis further confirmed postsynaptic localization of IFT proteins (Fig. 8, E–G). IFT20, -52, and -57 were concentrated in the dendritic terminals of bipolar and horizontal

Published April 5, 2010

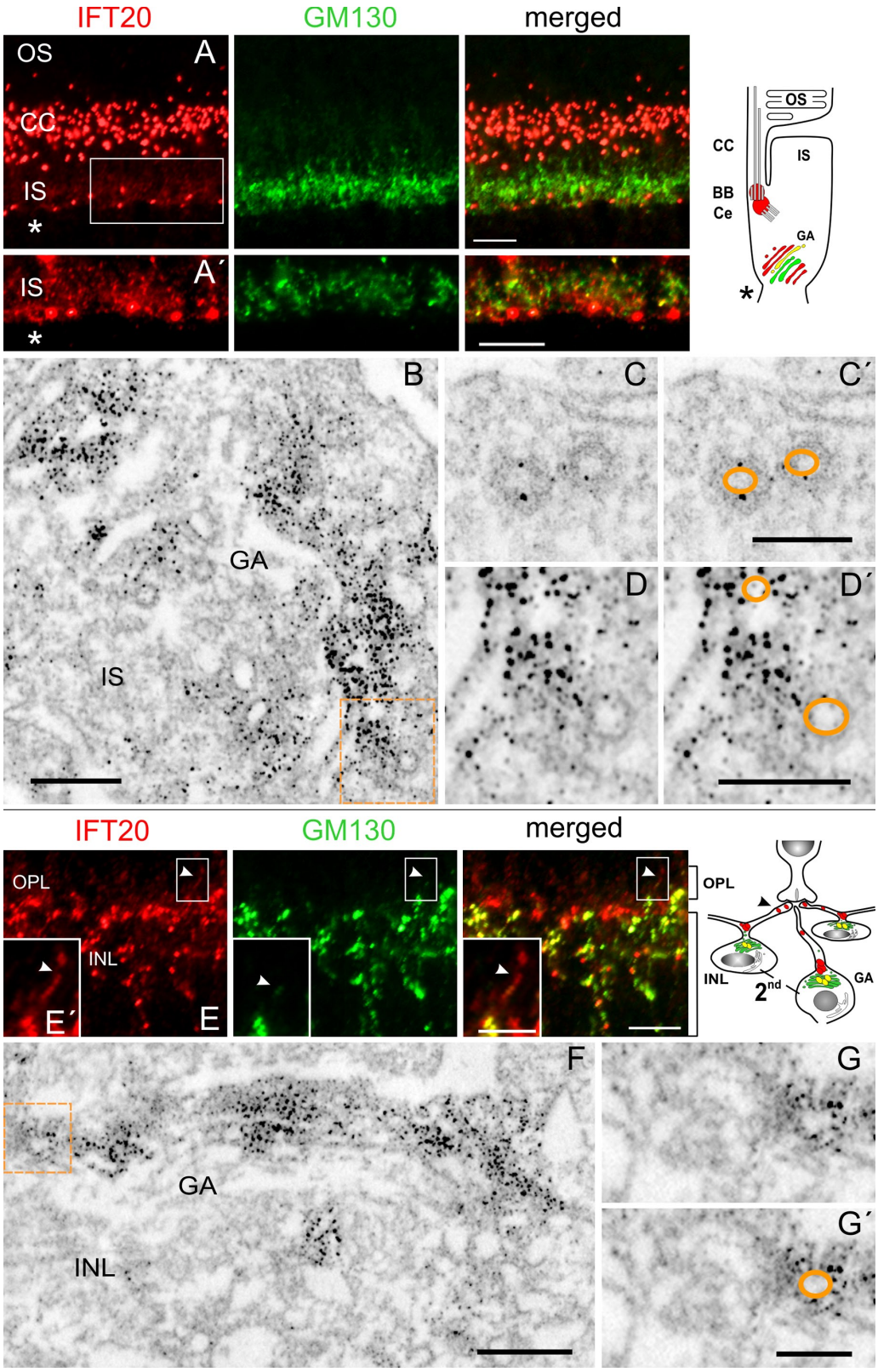

Figure 7. **Subcellular localization of IFT20 at the GA in neurons of the mouse retina.** (A–D) Localization of IFT20 in the GA of photoreceptor cells. (A) Indirect immunofluorescence of a double labeling with anti-IFT20 and anti-GM130, a marker for the GA. (A′) Higher magnification image of the indicated part (white rectangle) in A. Merged images reveal partial colocalization of IFT20 and GM130 in the GA of the IS summarized in the cartoon on the right. Asterisks indicate the apical part of the ONL. (B) Electron micrographs of anti-IFT20 immunolabeling in a cross section through the GA in the IS of a mouse photoreceptor cell. IFT20 is associated with the membrane stacks of the GA. (C and D) Anti-IFT20 labels vesicle-like structures, probably representing post-Golgi vesicles, highlighted by orange circles in C′ and D′. D and D′ are higher magnifications of B (orange rectangle). (E–G) Localization of IFT20 in the GA of secondary retinal neurons (2nd). (E) Indirect immunofluorescence of double labeling with anti-IFT20 and anti-GM130 in the OPL and

Published April 5, 2010

cells (Fig. 8, E–G). In addition to these IFT proteins, KIF17 was located in these postsynapses (Fig. 8 H). In no case were the presynaptic terminals of rod and cone photoreceptors stained by antibodies against IFT proteins. Furthermore, IFT20, -52, and -57 were also detected in the cytoplasm of dendritic processes of the retinal secondary neurons (Fig. 9, B–D) where the IFT proteins were clustered at vesicle-like structures (Fig. 9, B′–D′).

Discussion

In this study, we investigated the subcellular spatial distribution of five IFT particle proteins of complex A and B in cells of the mammalian retina. The applied preembedding labeling method for immunoelectron microscopy enabled spatial mapping of IFT proteins to subcellular compartments of cells and subciliary compartments of a primary cilium for the first time. In addition, it allowed the identification of ciliary cargo vesicles associated with the IFT proteins (Sedmak et al., 2009). Our results confirm the central function of IFT molecules in ciliary transport and further strengthen their role in transport processes in the cytoplasm of ciliated cells but also of nonciliated cells.

IFT proteins participate in all modules of the molecular transport destined to photoreceptor cilia

We provide evidence that IFT particle proteins participate in all principle modules of the transport destined to the photoreceptor cilia necessary for ciliogenesis (photoreceptor OS formation) and the maintenance of the light-receptive OS (Fig. 10 A). Localization of IFT20 in the GA and its association with transport vesicles in the cytoplasm of all retinal cell types and of the adjacent RPE support the model of the general nonciliary function of IFT20 as a molecular mediator between the sorting machinery of the GA, the vesicular transport of cilia components, and their delivery to the ciliary base (Follit et al., 2006, 2008). In the GA, IFT20 is thought to be anchored to Golgi membranes by the golgin protein GMAP210, and after vesicle budding, IFT20 marks the ciliary-destined vesicles that translocate from the Golgi to the base of the cilium, where IFT20 binds to other complex B subunits (Follit et al., 2006, 2008; Omori et al., 2008).

In photoreceptor cells, we monitored IFT20-associated vesicles on their track through the IS to the base of the CC. In the defined periciliary compartment, all five IFT proteins studied were abundantly concentrated and associated with cargo vesicles. These findings affirm previous results (Pazour et al., 2002; Luby-Phelps et al., 2008) and thereby support the hypothesis of the assembly and arrangement of IFT complexes at the base of cilia and flagella (Rosenbaum and Witman, 2002; Pedersen and Rosenbaum, 2008). As in other ciliary systems, all IFT molecules were found to be associated with Golgi-derived transport vesicles in photoreceptor cells. Previous experiments showed that the visual pigment rhodopsin is transported along microtubules by cytoplasmic dynein to the periciliary apical membrane of the IS (Fig. 10 A; Tai et al., 1999). At the ciliary base of photoreceptors, the cargo is transferred from the module of the cytoplasmic IS transport to the module of ciliary delivery, in particular to the ciliary IFT system (Papermaster, 2002; Roepman and Wolfrum, 2007). This transfer of membrane cargo to the specialized periciliary membrane domain is in principle an exocytotic process. The certain involvement of IFT molecules in this process supports the hypothesis that the evolution of eukaryotic cilia and in particular the IFT system is originated from the exocytotic system in ancestral nonciliated cells (Avidor-Reiss et al., 2004; Jékely and Arendt, 2006). Nevertheless, present immunoelectron microscopy data revealed slightly different localizations of IFT proteins in this periciliary region (Fig. 10 A): IFT57, -88, and -140 were found beneath the groove formed by the transition of the ciliary membrane and the plasma membrane. In contrast, IFT20 and -52 were located in the apical extension of the IS. The latter region we recently identified as a periciliary target membrane for ciliary-destined transport vesicles in mammalian photoreceptor cells (Maerker et al., 2008). The differential distribution of IFT protein subsets may depend on the sequential assembly of IFT particles for the delivery into the cilium. However, because there is no overlap between the membrane localization of the two IFT protein subsets, they may be associated with different ciliary cargoes, which are independently delivered to different target zones in the periciliary compartment. In photoreceptor cells, different transport routes through the IS were recently suggested for different OS cargoes (Karan et al., 2008; Bhowmick et al., 2009), making different target zones in the IS plausible.

In addition to their abundant concentration at the ciliary base, IFT proteins were found in the distinct parts of the primary cilium of photoreceptors: in the BB, the CC, the basal OS, and the axoneme (Fig. 1). In the region of the BB, all IFT proteins were present and associated with cargo vesicles. In the CC, IFT52, -57, -88, and -140 were detected alongside the microtubule doublets, but IFT20 was absent. This confirms previous studies and supports the hypothesis that the first set of IFT proteins participates in the molecular cargo trafficking or is transported as cargo (in the case of complex A component IFT140, which is thought to be involved in retrograde IFT) through the CC (Rosenbaum et al., 1999; Baker et al., 2004; Insinna and Besharse, 2008; Insinna et al., 2008, 2009; Krock and Perkins, 2008; Luby-Phelps et al., 2008; Pedersen and Rosenbaum, 2008; Pigino et al., 2009). The faint decoration of the IFT proteins in the shaft of the CC by immunofluorescence and immunoelectron microscopy may reflect the velocity of the IFT particles as they pass through the CC. The concentration of IFT57, -88, and -140 at the base of the OS indicates a certain role of these IFT proteins in the formation of novel photosensitive

the INL. (E′) Higher magnification of a dendritic extension (arrowheads) indicated in E (white rectangles). Merged images reveal partial colocalization of IFT20 and GM130 in dendritic extension and in the GA of second retinal neurons outlined in the cartoon on the right. (F) Electron micrograph of anti-IFT20 immunolabeling in a cross section through the GA of second neurons in the INL. IFT20 associates with the membranes stacks of the GA of horizontal and bipolar cells. (G) Higher magnification of F (orange rectangle). IFT20 clusters at vesicle-like structures (post-Golgi vesicles), highlighted by the orange circle in G′. Ce, centriole. Bars: (A, A′, and E) 5 µm; (B) 0.4 µm; (C, C′, G, and G′) 0.1 µm; (D, D′, and F) 0.2 µm; (E′) 2.5 µm.

Published April 5, 2010

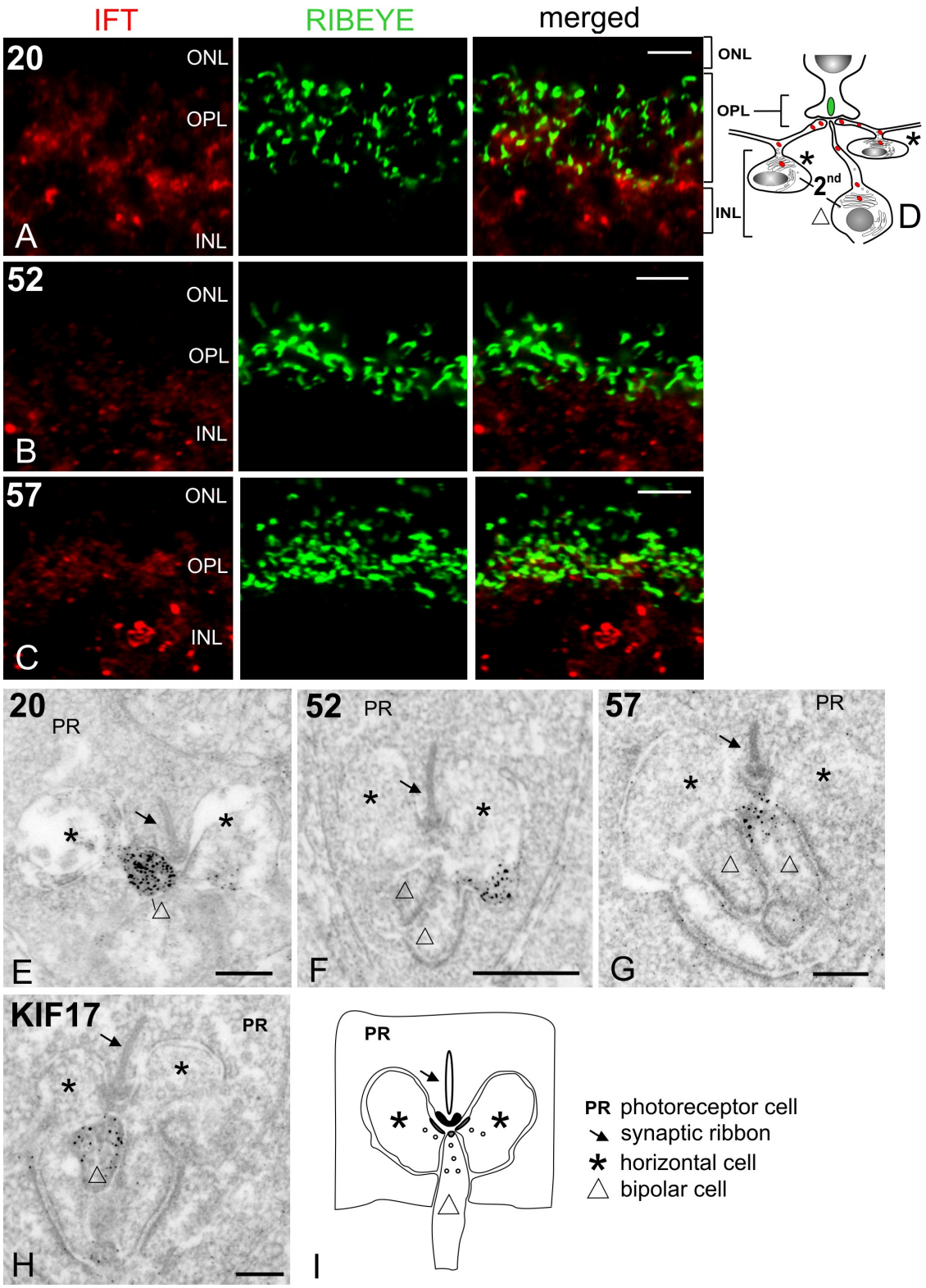

Figure 8. **Postsynaptic localization of IFT20, -52, and -57 and KIF17 in OPL synapses.** (A–C) Indirect immunofluorescence double labeling by antibodies to IFT20, -52, and -57 and RIBEYE, a marker for the presynaptic region of photoreceptor cell ribbon synapses in cryosections through mouse retinas. Merged images reveal no colocalization of RIBEYE and IFT proteins. (D) Cartoon of postsynaptic localization of IFT proteins in secondary retinal neurons (2nd), bipolar cells (triangle), and horizontal cells (asterisks). (E–G) Electron micrographs of immunolabeling of IFT20, -52, and -57 in the OPL synapses between photoreceptor cells (PR) and bipolar cells (triangles) and horizontal cells (asterisks). (H) Electron micrograph of anti-KIF17 immunolabeling in the OPL synapses. (I) Cartoon of the organization of a rod ribbon synapse contact to bipolar cells (triangle) and horizontal cells (asterisks). Arrows indicate synaptic ribbons in photoreceptor cells. IFT proteins and KIF17 are restricted to the postsynaptic terminals of dendritic processes of second retinal neurons. Bars: (A and B) 3 µm; (C) 5 µm; (E–H) 0.2 µm.

Published April 5, 2010

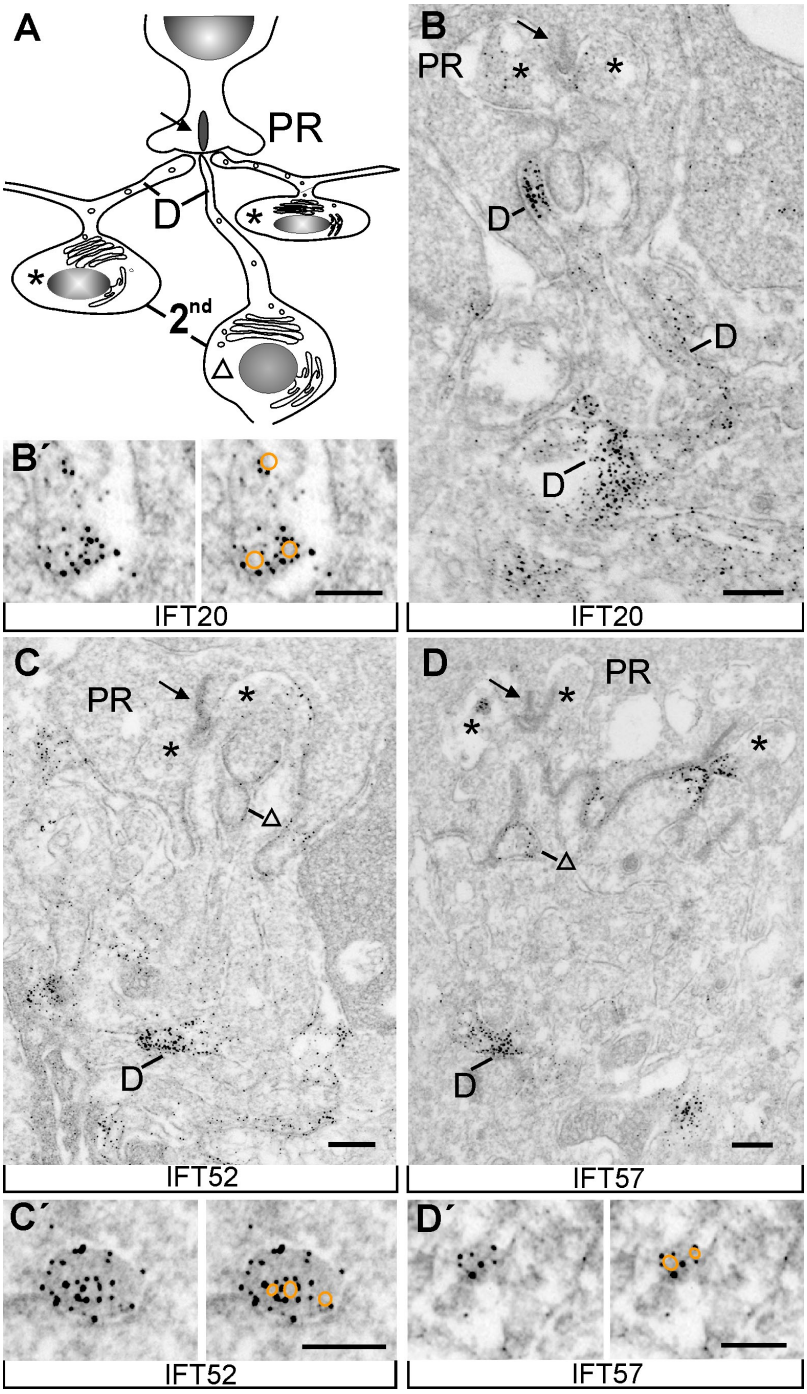

Figure 9. **Localization of IFT20, -52, and -57 in dendritic processes of secondary retinal neurons.** (A) Cartoon of the organization of an OPL synapse connection between a rod photoreceptor cell (PR) and the secondary retinal neurons (2nd), bipolar cells (triangle), and horizontal cells (asterisks). D, dendritic processes. (B–D) Electron micrographs of immunolabeling of IFT20, -52, and -57 in the OPL of mouse retinas. All three IFT proteins are decorated in dendritic processes of second neurons. (B′–D′) High magnification details of B–D indicating the association of IFT20, -52, and -57 with vesicle-like structures highlighted by orange circles. Arrows indicate the synaptic ribbon, and triangles and asterisks highlight bipolar and horizontal cells, respectively. Bars: (B–D) 0.2 µm; (B′–D′) 0.1 µm.

membranous disks. All de novo synthesized disk compounds are shipped through the CC, unloaded from their transport carriers (e.g., kinesin-II–driven IFT particles), and incorporated into the newly formed disks at the OS base. Although the molecular mechanism is currently still under debate, there is evidence that endocytosis of membrane vesicles is involved in the formation of nascent disk membranes at the base of the OS (Usukura and Obata, 1995; Chuang et al., 2007; unpublished data).

In the photoreceptor axoneme, which extends from the CC and projects deep into the OS (Liu et al., 2004; Insinna and Besharse, 2008), only IFT88 and -140 were detected. This suggests that only a subset of IFT proteins participates in IFT processes associated with the transport of cargo that is not incorporated into the nascent disks at the OS base and translocates along the microtubules of the axoneme in the OS. The axonemal localization and function of IFT88 is in agreement with a correct differentiation of the CC but failure of a proper OS formation in photoreceptor cells of mice carrying the hypomorphic mutation in IFT88 ($Tg737^{orpk}$; Pazour et al., 2002; Baker et al., 2004). Because most components of the photosensitive disks are incorporated into the nascent disks already at base of the OS, only a subset of OS molecules has to be distributed more apically as cargo for the transport machinery of the axoneme (Roepman and Wolfrum, 2007). Such cargoes, distributed

Published April 5, 2010

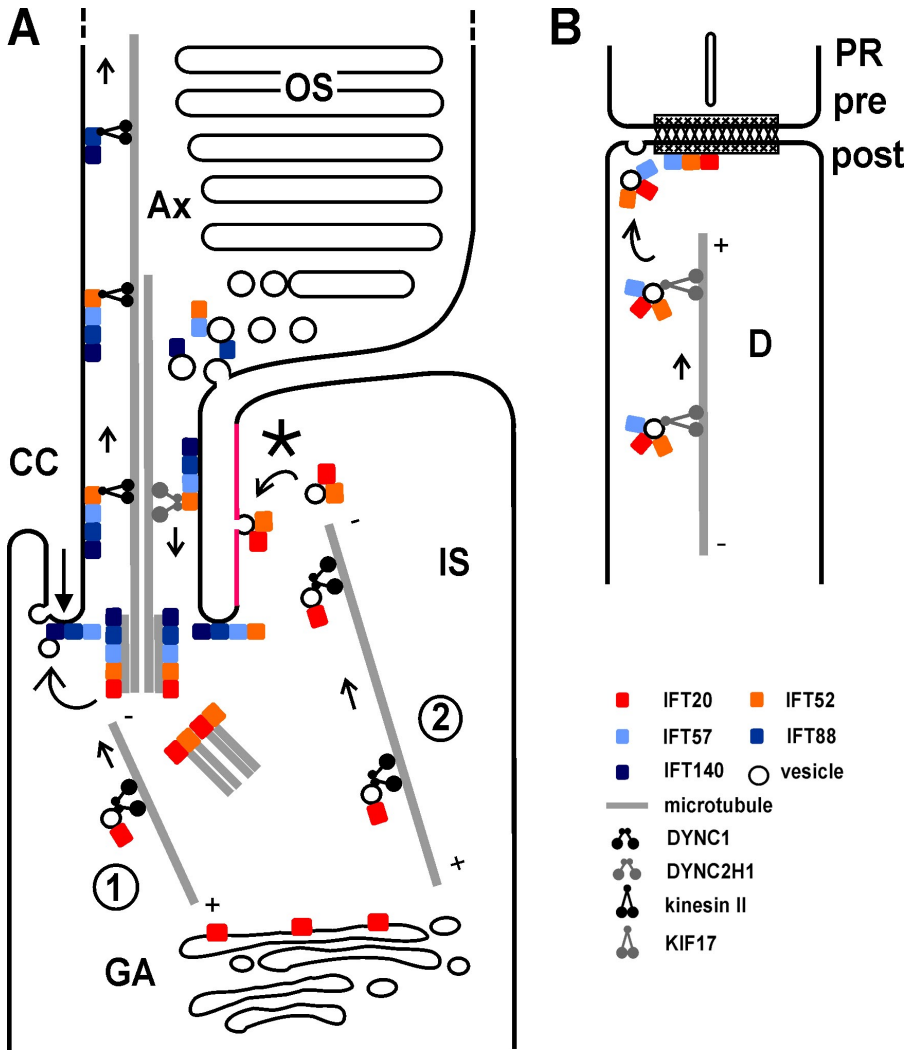

Figure 10. **Models of processes associated with IFT proteins in retinal neurons.** (A) IFT in photoreceptor cells. On its destination to the OS, cytoplasmic dynein 1 (DYNC1) mediates the transport of cargo vesicles along microtubules from the GA on route 1 to the base of the CC (BB region) and on route 2 to the periciliary extension (asterisk) of the IS. In the IS, IFT20 is associated with cargo vesicles on both routes. Route 1 vesicles are directed to the periciliary groove (big arrow) in the periphery of the BB where they associate with IFT57, -88, and -140 and fuse with the periciliary groove membrane. Route 2 vesicles directed to the periciliary IS extension are associated with IFT20 and -52 and fuse with the periciliary target membrane (red). Subsequently, kinesin-II family motors mediate transport of route 1 and 2 cargoes attached to IFT particles containing IFT52, -57, -88, and -140 but not IFT20 through the CC. At the OS base, the majority of IFT proteins dissociate from the cargo, which is incorporated into membranes of de novo organized OS disks. Further apical, IFT particles containing IFT88 and -140 but not IFT20, -52, and -57 are transported along axonemal microtubules. For retrograde transport, IFT particles are picked up by cytoplasmic dynein 2/1b (DYNC2H1). Ax, axoneme. (B) IFT in dendritic process of nonciliated secondary retinal neurons. In the dendritic processes (D) of second retinal neurons, cargo vesicles are transported by KIF17 to the dendritic postsynaptic terminal (post). Dendritic IFT particles contain IFT20, -52, and -57. At the dendritic terminal, IFT particles dissociate from their cargo, which is incorporated into the postsynaptic membrane. PR, photoreceptor cell; pre, presynapse.

in the OS independently from the disk neogenesis, are, for example, arrestin and the visual G-protein transducin, which light-dependently cycle between the inner and the OS (Calvert et al., 2006). Recent data indicate that these bidirectional movements are dependent on the axonemal microtubule track (Peterson et al., 2005; Reidel et al., 2008; Orisme et al., 2010). The IFT complex B protein IFT88 may contribute to the translocation of both signaling molecules into the OS during photoreceptor adaptation, whereas, in the clearance of transducin and arrestin from the OS, the IFT complex A compound IFT140 may participate. Our findings confirm previous observations in other cilia and flagella, in which sets of IFT components were also found to be sequentially organized or spatially distributed in ciliary subcompartments (Evans et al., 2006; Ou et al., 2007; Lee et al., 2008).

IFT20 is not a component of the IFT core complex B in photoreceptor cilia

In contrast to all other IFT molecules investigated, we did not find IFT20 in the CC of photoreceptor cells. The present subcellular mapping by the sophisticated light and electron microscopy consistently revealed that IFT20 is restricted to the periciliary cytoplasm of the apical IS and the BB but is neither present in the CC nor in more apical sections of the photoreceptor cilium in all species investigated. This is in contrast to previous studies suggesting a ciliary localization of IFT20 (Pazour et al., 2002; Follit et al., 2006, 2008, 2009). Follit et al. (2006) discuss that the ciliary detection is dependent on the fixation protocol because of epitope masking after fixation, which our control experiments did not confirm. Nevertheless, all published immunofluorescence data on the intrinsic IFT20 ciliary staining are not convincing, and a solid ciliary localization of IFT20 is only found after IFT20 overexpression (Follit et al., 2006, 2008). It is possible that the high sensitivity of the elaborated techniques used in this study is still not sensitive enough for the detection of IFT20 in photoreceptor cilia or that IFT20 epitopes are not accessible for the antibodies because of variations in the composition and position of the IFT molecules in the particles. Nevertheless, we believe that IFT20 is not present in photoreceptor cilia. IFT20's absence from the ciliary IFT complex B is supported by the lack of IFT20 in IFT particle fractions of gradients derived from photoreceptors (Baker et al., 2003) and unpublished data on proteomic dissection of the complex B in cultured mammalian cells. Furthermore, the analysis of complex B composition in *Chlamydomonas* demonstrated that IFT20 is linked to a complex B core by weak and

Published April 5, 2010

transient interactions (Lucker et al., 2005), which might play a role in the assembly and rearrangements of IFT protein complexes at the flagellum base (Iomini et al., 2001). In fact, IFT particles containing IFT20 are present in the apical IS and the BB, which is consistent with previously obtained data (Pazour et al., 2002; Follit et al., 2006, 2008) that promote a mediator role of IFT20 between the Golgi system and the cargo delivery to target membranes.

Evidence for a novel IFT system in dendrites of nonciliated retinal neurons

Besides the presence of IFT20 in the GA, IFT systems were recently found in nonciliated cells, associated with exocytosis at the immune synapse required for T cell interaction with antigen-presenting cells (Finetti et al., 2009; Baldari and Rosenbaum, 2010). In the mammalian retina, a weak immunoreactivity for IFT proteins present in the OPL was construed as a localization of IFT proteins in the photoreceptor synaptic terminals (Pazour et al., 2002). The latter finding, together with IFT-associated kinesin-II localization at these synapses (Muresan et al., 1999), raised the possibility of a function of IFT proteins in presynaptic terminals (Pazour et al., 2002). Nevertheless, in this study, we show that IFT20, -52, and -57 proteins are localized not in the presynaptic terminals of photoreceptor cells but in the postsynaptic terminals of the bipolar and horizontal cells. Double immunofluorescence staining with synaptic markers and preembedding labeling of IFT molecules conclusively revealed localization of the three IFT molecules in the postsynaptic dendritic terminals and dendritic shafts of secondary retinal neurons. This spatial distribution and the association of these IFT molecules with cytoplasmic membrane vesicles suggest participation of an IFT system at the vesicular transport to the specialized membrane of the postsynaptic dendritic terminal (Fig. 10 B). It has been demonstrated that the kinesin-II family member KIF17 navigates large protein complexes containing subunits of neurotransmitter receptors to the postsynaptic terminals (Setou et al., 2000; Guillaud et al., 2003). In secondary retinal neurons, KIF17 regulates the dendritic transport of glutamate receptor subunits to the postsynaptic membrane (Qin and Pourcho, 2001; Kayadjanian, et al., 2007). It is notable that the specific targeting of neurotransmitter receptors is critically important for plasticity of the postsynaptic terminal and might be a regulatory point for synaptic plasticity and neuronal morphogenesis. KIF17 has been found as an alternative kinesin motor to kinesin-II in IFT (Signor et al., 1999b). In the vertebrate retina, KIF17 was identified as part of a protein complex containing IFT20 and -57, which is essential for photoreceptor OS development (Insinna et al., 2008, 2009). Our present data indicate that the dendritic processes of secondary retinal neurons contain a nonciliary IFT protein complex that includes IFT20, -52, and -57 and KIF17 but neither IFT88 nor the heterotrimeric kinesin-II (Fig. 10 B). Thus, the nonciliary dendritic IFT complex differs in its composition from the one recently described for the immune synapse (Finetti et al., 2009). We reason that IFT protein complexes are modularly composed and that their defined arrangement may be cell specific and/or dependent on a particular role of the IFT protein complex in intracellular membrane trafficking to selective target membranes.

In conclusion, a major implication of the present data is that IFT protein complexes contain different IFT proteins in different compartments of photoreceptor primary cilia. In addition, we demonstrate that IFT20 is more a mediator between the cargo sorting in the Golgi, the cytoplasmic cargo trafficking, and the delivery into the cilium than an intrinsic ciliary component. Furthermore, we identified a nonciliary IFT system by mapping IFT proteins to dendrites of retinal neurons. Our data support new perspectives on IFT function beyond its well-established roles in cilia assembly, maintenance, and sensory function of cilia and flagella.

Materials and methods

Animals, tissue dissection, and human tissue

All experiments conformed to the statement by the Association for Research in Vision and Ophthalmology regarding the care and use of animals in research. Mature C57BL/6J mice were maintained on a 12-h light–dark cycle, with food and water ad libitum. After the sacrifice of animals, eyeballs were dissected for further analyses. Bovine eyes were obtained from the local slaughter house. Human eyes (female, age 78, 13 h postmortem) were donated (Department of Ophthalmology, University Medical Center of the Johannes Gutenberg University Mainz). Informed consent was obtained for subjects; procedures adhered to the Declaration of Helsinki and were approved by the local review board. Retina was isolated from eyeball and further processed for immunofluorescence analysis as described in Immunofluorescence microscopy.

Antibodies and fluorescent dyes

Antisera against IFT20, -52, -57, -88, and -140 proteins were raised in rabbit, and affinity-purified antibodies used in this study were previously characterized (Pazour et al., 2002; Baker et al., 2003; Follit et al., 2006) and provided by G.J. Pazour (University of Massachusetts Medical School, Worcester, MA). Monoclonal antibodies to centrin-3 were used as a molecular marker for the ciliary apparatus of photoreceptors (Trojan et al., 2008). Monoclonal mouse antibodies to RIBEYE (CtBP2) and to the Golgi-resident GM130 were purchased from BD and were previously used as a cis and medial Golgi marker in photoreceptor cells by Mazelova et al. (2009). Polyclonal rabbit anti-KIF17 was obtained from Abcam and previously used in Insinna et al. (2009). Anti-RP1 antibody raised in chicken was a gift from E.A. Pierce (University of Pennsylvania School of Medicine, Philadelphia, PA; Liu et al., 2002). Secondary antibodies Alexa Fluor 488 or 568 (Invitrogen), IRDye 680 or 800 (Rockland), donkey anti–rabbit horse conjugated with reddish peroxidase (GE Healthcare), and biotinylated secondary antibodies (Vector Laboratories) were used. Nuclear DNA was stained by 1 µg/µl DAPI (Sigma-Aldrich).

Western blot analyses

For Western blot analyses, isolated mouse retinas and testes were homogenized in buffer containing a protease inhibitor cocktail (Roche). Specimens were extracted in modified radioimmunoprecipitation assay buffer (50 mM Tris-HCl, 150 mM NaCl, 0.1% SDS, 2 mM EDTA, 1% NP-40, 0.5% Na deoxycholate, 1 mM Na vanadate, and 30 mM Na-pyrophosphate, pH 7.4). For denaturing gel electrophoresis, samples were mixed with SDS-PAGE sample buffer (62.5 mM Tris-HCl, 10% glycerol, 2% SDS, 5% mercaptoethanol, 1 mM EDTA, and 0.025 mM bromophenol blue, pH 6.8). Protein extracts from retinas and testes were separated on 12% or 15% polyacrylamide gels, respectively, and transferred onto polyvinylidene difluoride membranes (Millipore). The membrane was blocked with blocking reagent (AppliChem) or nonfat dry milk (AppliChem) for 2 h at room temperature. Immunoreactivity was detected by the appropriate primary and corresponding secondary antibodies using an infrared imaging system (Odyssey; LI-COR Biosciences) for AppliChem-blocked membrane or the chemiluminescence detection system (ECL Plus Western blotting detection system; GE Healthcare) for nonfat dry milk–blocked membrane. In the latter case, ECL-exposed and developed x-ray films were scanned using a Duoscan T2500 (Agfa-Gevaert), and images were processed in Photoshop CS (Adobe Systems).

Immunofluorescence microscopy

Eyes of adult mice were placed in tissue-freezing medium (Leica) enclosed by boiled-liver block and cryofixed in melting isopentane (Wolfrum, 1991). Mouse eyes were sectioned in 10-µm cryosections at −20°C in a cryostat (HM 560 Cryo-Star; MICROM). Cryosections were placed on poly-L-lysine–precoated coverslips. Some cryosections were additionally fixed for 1 min in cold methanol containing 0.05% EGTA and washed with PBS. After incubation with 0.01% Tween 20 in PBS, PBS-washed sections were incubated with blocking solution (0.5% cold-water fish gelatin and 0.1% ovalbumin in PBS), followed by overnight incubation with primary antibodies, and diluted in blocking solution at 4°C. Washed cryosections were incubated with Alexa Fluor–conjugated secondary antibodies in PBS with DAPI. After PBS washes, sections were mounted in Mowiol 4.88 (Hoechst) and analyzed in a microscope (LEITZ DMRB; Leica) through a 63× NA 1.32 HCX Plan-Apochromat and a 100× NA 1.3 Plan-Fluotar oil objective lens. Images were obtained with a charge-coupled device camera (ORCA ER; Hamamatsu Photonics). Image acquisition was always performed at the same gain and exposure settings. Image contrast was adjusted offline with Photoshop CS using different tools, including color correction and pixel resampling.

Immunoelectron microscopy

For immunoelectron microscopy, a recently introduced protocol was applied (Maerker et al., 2008; Sedmak et al., 2009). During fixation of isolated mouse eyes in 4% PFA in Sorensen buffer (0.1 M $Na_2HPO_4{\cdot}2H_2O$ and 0.1 M KH_2PO_4, pH 7.4), eyes were perforated, and lenses were removed. Washed retinas were dissected from eye cups and infiltrated with 10 and 20% sucrose in Sorensen buffer, followed by incubation in buffered 30% sucrose overnight. After four cycles of freezing in liquid nitrogen and thawing at 37°C, retinas were washed in PBS and embedded in buffered 2% Agar (Sigma-Aldrich). Agar blocks were sectioned with a Vibratome (VT 1000 S; Leica) in 50-µm slices. Vibratome sections were blocked in 10% normal goat serum and 1% bovine serum albumin in PBS and subsequently incubated with primary antibodies against IFT proteins for 4 d at 4°C. After washing with PBS, the appropriate biotinylated secondary antibodies were applied to the sections. After PBS washes, antibody reactions were visualized by a Vectastain ABC kit (Vector Laboratories) according to the manufacturer's instructions. The Vectastain ABC kit provides the avidin-biotin HRP complex (ABC), which binds the biotin-conjugated secondary antibodies. The immunocomplex was visualized by adding 0.01% hydrogen peroxide to 0.05 M DAB solution. In this reaction, DAB was oxidized, converting DAB into insoluble polymers. Subsequently, stained retinas were fixed in 2.5% glutaraldehyde in 0.1 M cacodylate buffer, pH 7.4, and DAB precipitates were silver enhanced, applying a modified protocol by Leranth and Pickel (1989) followed by postfixation in 0.5% OsO_4 in 0.1 M cacodylate buffer on ice. Dehydrated specimens were flat-mounted between two sheaths of ACLAR-films (Ted Pella, Inc.) in Araldite resin. Ultrathin sections were analyzed in a transmission electron microscope (Tecnai 12 BioTwin; FEI) using different magnifications ranging from 11,500 to 26,500. Images were obtained with a charge-coupled device camera (SIS Megaview3; Surface Imaging Systems) acquired by analSIS (Soft Imaging System) and processed with Photoshop CS.

Online supplemental material

Fig. S1 presents Western blot analyses of murine retinas and testes demonstrating the retinal expression and monospecificity of the antibodies to the different IFT proteins used. Fig. S2 shows analyses of the distribution of IFT proteins in subcellular compartments of ocular cells. Fig. S3 shows analyses of the spatial distribution of IFT proteins in retinal cells of nonrodent mammals. Fig. S4 demonstrates no differences in anti-IFT20 indirect immunofluorescence staining in fixed and unfixed mouse retinas. Online supplemental material is available at http://www.jcb.org/cgi/content/full/jcb.200911095/DC1.

We thank Elisabeth Sehn, Ulrike Maas, and Gabi Stern-Schneider for excellent technical assistance, Drs. Martin Latz, Kerstin Nagel-Wolfrum, Nora Overlack, and Michel van Wyk for discussions and critical reading, and Drs. Gregory J. Pazour and Eric Pierce for providing antibodies. Furthermore, we thank Dr. Joel Rosenbaum for the inspiration and encouragement to perform this study.

This work was supported by grants from the Deutsche Forschungsgemeinschaft (to U. Wolfrum), Forschung contra Blindheit (to U. Wolfrum), ProRetina Deutschland (to U. Wolfrum), the FAUN-Stiftung (to U. Wolfrum), and the Rheinland-Pfalz Graduiertenförderung (to T. Sedmak).

Submitted: 17 November 2009
Accepted: 9 March 2010

References

Avidor-Reiss, T., A.M. Maer, E. Koundakjian, A. Polyanovsky, T. Keil, S. Subramaniam, and C.S. Zuker. 2004. Decoding cilia function: defining specialized genes required for compartmentalized cilia biogenesis. *Cell*. 117:527–539. doi:10.1016/S0092-8674(04)00412-X

Baker, S.A., K. Freeman, K. Luby-Phelps, G.J. Pazour, and J.C. Besharse. 2003. IFT20 links kinesin II with a mammalian intraflagellar transport complex that is conserved in motile flagella and sensory cilia. *J. Biol. Chem.* 278:34211–34218. doi:10.1074/jbc.M300156200

Baker, S.A., G.J. Pazour, G.B. Witman, and J.C. Besharse. 2004. Photoreceptors and intraflagellar transport. In *Photoreceptor cell biology and inherited retinal degenerations*. Recent Advances in Human Biology, vol. 10. D.S. Williams, editor. World Scientific, Singapore. 109–132.

Baldari, C.T., and J. Rosenbaum. 2010. Intraflagellar transport: it's not just for cilia anymore. *Curr. Opin. Cell Biol.* 22:75–80. doi:10.1016/j.ceb.2009.10.010

Beech, P.L., K. Pagh-Roehl, Y. Noda, N. Hirokawa, B. Burnside, and J.L. Rosenbaum. 1996. Localization of kinesin superfamily proteins to the connecting cilium of fish photoreceptors. *J. Cell Sci.* 109:889–897.

Besharse, J.C., and C.J. Horst. 1990. The photoreceptor connecting cilium - a model for the transition zone. *In* Ciliary and Flagellar Membranes. R.A. Bloodgood, editor. Plenum, New York. 389–417.

Bhowmick, R., M. Li, J. Sun, S.A. Baker, C. Insinna, and J.C. Besharse. 2009. Photoreceptor IFT complexes containing chaperones, guanylyl cyclase 1 and rhodopsin. *Traffic*. 10:648–663. doi:10.1111/j.1600-0854.2009.00896.x

Calvert, P.D., K.J. Strissel, W.E. Schiesser, E.N. Pugh Jr., and V.Y. Arshavsky. 2006. Light-driven translocation of signaling proteins in vertebrate photoreceptors. *Trends Cell Biol.* 16:560–568. doi:10.1016/j.tcb.2006.09.001

Chuang, J.Z., Y. Zhao, and C.H. Sung. 2007. SARA-regulated vesicular targeting underlies formation of the light-sensing organelle in mammalian rods. *Cell*. 130:535–547. doi:10.1016/j.cell.2007.06.030

Cole, D.G. 2003. The intraflagellar transport machinery of *Chlamydomonas reinhardtii*. *Traffic*. 4:435–442. doi:10.1034/j.1600-0854.2003.t01-1-00103.x

Cole, D.G., D.R. Diener, A.L. Himelblau, P.L. Beech, J.C. Fuster, and J.L. Rosenbaum. 1998. *Chlamydomonas* kinesin-II–dependent intraflagellar transport (IFT): IFT particles contain proteins required for ciliary assembly in *Caenorhabditis elegans* sensory neurons. *J. Cell Biol.* 141:993–1008. doi:10.1083/jcb.141.4.993

Deane, J.A., D.G. Cole, E.S. Seeley, D.R. Diener, and J.L. Rosenbaum. 2001. Localization of intraflagellar transport protein IFT52 identifies basal body transitional fibers as the docking site for IFT particles. *Curr. Biol.* 11:1586–1590. doi:10.1016/S0960-9822(01)00484-5

Evans, J.E., J.J. Snow, A.L. Gunnarson, G. Ou, H. Stahlberg, K.L. McDonald, and J.M. Scholey. 2006. Functional modulation of IFT kinesins extends the sensory repertoire of ciliated neurons in *Caenorhabditis elegans*. *J. Cell Biol.* 172:663–669. doi:10.1083/jcb.200509115

Finetti, F., S.R. Paccani, M.G. Riparbelli, E. Giacomello, G. Perinetti, G.J. Pazour, J.L. Rosenbaum, and C.T. Baldari. 2009. Intraflagellar transport is required for polarized recycling of the TCR/CD3 complex to the immune synapse. *Nat. Cell Biol.* 11:1332–1339. doi:10.1038/ncb1977

Follit, J.A., R.A. Tuft, K.E. Fogarty, and G.J. Pazour. 2006. The intraflagellar transport protein IFT20 is associated with the Golgi complex and is required for cilia assembly. *Mol. Biol. Cell*. 17:3781–3792. doi:10.1091/mbc.E06-02-0133

Follit, J.A., J.T. San Agustin, F. Xu, J.A. Jonassen, R. Samtani, C.W. Lo, and G.J. Pazour. 2008. The Golgin GMAP210/TRIP11 anchors IFT20 to the Golgi complex. *PLoS Genet.* 4:e1000315. doi:10.1371/journal.pgen.1000315

Follit, J.A., F. Xu, B.T. Keady, and G.J. Pazour. 2009. Characterization of mouse IFT complex B. *Cell Motil. Cytoskeleton*. 66:457–468. doi:10.1002/cm.20346

Guillaud, L., M. Setou, and N. Hirokawa. 2003. KIF17 dynamics and regulation of NR2B trafficking in hippocampal neurons. *J. Neurosci.* 23:131–140.

Hou, Y., H. Qin, J.A. Follit, G.J. Pazour, J.L. Rosenbaum, and G.B. Witman. 2007. Functional analysis of an individual IFT protein: IFT46 is required for transport of outer dynein arms into flagella. *J. Cell Biol.* 176:653–665. doi:10.1083/jcb.200608041

Insinna, C., and J.C. Besharse. 2008. Intraflagellar transport and the sensory outer segment of vertebrate photoreceptors. *Dev. Dyn.* 237:1982–1992. doi:10.1002/dvdy.21554

Insinna, C., N. Pathak, B. Perkins, I. Drummond, and J.C. Besharse. 2008. The homodimeric kinesin, Kif17, is essential for vertebrate photoreceptor sensory outer segment development. *Dev. Biol.* 316:160–170. doi:10.1016/j.ydbio.2008.01.025

Insinna, C., M. Humby, T. Sedmak, U. Wolfrum, and J.C. Besharse. 2009. Different roles for KIF17 and kinesin II in photoreceptor development and maintenance. *Dev. Dyn.* 238:2211–2222. doi:10.1002/dvdy.21956

Iomini, C., V. Babaev-Khaimov, M. Sassaroli, and G. Piperno. 2001. Protein particles in *Chlamydomonas* flagella undergo a transport cycle consisting of four phases. *J. Cell Biol.* 153:13–24. doi:10.1083/jcb.153.1.13

Jékely, G., and D. Arendt. 2006. Evolution of intraflagellar transport from coated vesicles and autogenous origin of the eukaryotic cilium. *Bioessays*. 28:191–198. doi:10.1002/bies.20369

Karan, S., J.M. Frederick, and W. Baehr. 2008. Involvement of guanylate cyclases in transport of photoreceptor peripheral membrane proteins. *Adv. Exp. Med. Biol.* 613:351–359. doi:10.1007/978-0-387-74904-4_41

Kayadjanian, N., H.S. Lee, J. Piña-Crespo, and S.F. Heinemann. 2007. Localization of glutamate receptors to distal dendrites depends on subunit composition and the kinesin motor protein KIF17. *Mol. Cell. Neurosci.* 34: 219–230. doi:10.1016/j.mcn.2006.11.001

Kozminski, K.G., K.A. Johnson, P. Forscher, and J.L. Rosenbaum. 1993. A motility in the eukaryotic flagellum unrelated to flagellar beating. *Proc. Natl. Acad. Sci. USA*. 90:5519–5523. doi:10.1073/pnas.90.12.5519

Kozminski, K.G., P.L. Beech, and J.L. Rosenbaum. 1995. The *Chlamydomonas* kinesin-like protein FLA10 is involved in motility associated with the flagellar membrane. *J. Cell Biol.* 131:1517–1527. doi:10.1083/jcb .131.6.1517

Krock, B.L., and B.D. Perkins. 2008. The intraflagellar transport protein IFT57 is required for cilia maintenance and regulates IFT-particle-kinesin-II dissociation in vertebrate photoreceptors. *J. Cell Sci.* 121:1907–1915. doi:10.1242/jcs.029397

Lee, E., E. Sivan-Loukianova, D.F. Eberl, and M.J. Kernan. 2008. An IFT-A protein is required to delimit functionally distinct zones in mechanosensory cilia. *Curr. Biol.* 18:1899–1906. doi:10.1016/j.cub.2008.11.020

Leranth, C., and V.M. Pickel. 1989. Electron microscopic preembedding double immunostaining methods. *In* Neuroanatomical Tract-Tracing Methods 2. L. Heimer and L. Záborszky, editors. Plenum press, New York. 129–172.

Liu, Q., J. Zhou, S.P. Daiger, D.B. Farber, J.R. Heckenlively, J.E. Smith, L.S. Sullivan, J. Zuo, A.H. Milam, and E.A. Pierce. 2002. Identification and subcellular localization of the RP1 protein in human and mouse photoreceptors. *Invest. Ophthalmol. Vis. Sci.* 43:22–32.

Liu, Q., J. Zuo, and E.A. Pierce. 2004. The retinitis pigmentosa 1 protein is a photoreceptor microtubule-associated protein. *J. Neurosci.* 24:6427–6436. doi:10.1523/JNEUROSCI.1335-04.2004

Liu, Q., G. Tan, N. Levenkova, T. Li, E.N. Pugh Jr., J.J. Rux, D.W. Speicher, and E.A. Pierce. 2007. The proteome of the mouse photoreceptor sensory cilium complex. *Mol. Cell. Proteomics*. 6:1299–1317. doi:10.1074/mcp .M700054-MCP200

Luby-Phelps, K., J. Fogerty, S.A. Baker, G.J. Pazour, and J.C. Besharse. 2008. Spatial distribution of intraflagellar transport proteins in vertebrate photoreceptors. *Vision Res.* 48:413–423. doi:10.1016/j.visres.2007.08.022

Lucker, B.F., R.H. Behal, H. Qin, L.C. Siron, W.D. Taggart, J.L. Rosenbaum, and D.G. Cole. 2005. Characterization of the intraflagellar transport complex B core: direct interaction of the IFT81 and IFT74/72 subunits. *J. Biol. Chem.* 280:27688–27696. doi:10.1074/jbc.M505062200

Maerker, T., E. van Wijk, N. Overlack, F.F. Kersten, J. McGee, T. Goldmann, E. Sehn, R. Roepman, E.J. Walsh, H. Kremer, and U. Wolfrum. 2008. A novel Usher protein network at the periciliary reloading point between molecular transport machineries in vertebrate photoreceptor cells. *Hum. Mol. Genet.* 17:71–86. doi:10.1093/hmg/ddm285

Mazelova, J., N. Ransom, L. Astuto-Gribble, M.C. Wilson, and D. Deretic. 2009. Syntaxin 3 and SNAP-25 pairing, regulated by omega-3 docosahexaenoic acid, controls the delivery of rhodopsin for the biogenesis of cilia-derived sensory organelles, the rod outer segments. *J. Cell Sci.* 122:2003–2013. doi:10.1242/jcs.039982

Murcia, N.S., W.G. Richards, B.K. Yoder, M.L. Mucenski, J.R. Dunlap, and R.P. Woychik. 2000. The Oak Ridge Polycystic Kidney (orpk) disease gene is required for left-right axis determination. *Development*. 127:2347–2355.

Muresan, V., A. Lyass, and B.J. Schnapp. 1999. The kinesin motor KIF3A is a component of the presynaptic ribbon in vertebrate photoreceptors. *J. Neurosci.* 19:1027–1037.

Nakamura, N., C. Rabouille, R. Watson, T. Nilsson, N. Hui, P. Slusarewicz, T.E. Kreis, and G. Warren. 1995. Characterization of a cis-Golgi matrix protein, GM130. *J. Cell Biol.* 131:1715–1726. doi:10.1083/jcb.131.6.1715

Omori, Y., C. Zhao, A. Saras, S. Mukhopadhyay, W. Kim, T. Furukawa, P. Sengupta, A. Veraksa, and J. Malicki. 2008. Elipsa is an early determinant of ciliogenesis that links the IFT particle to membrane-associated small GTPase Rab8. *Nat. Cell Biol.* 10:437–444. doi:10.1038/ncb1706

Orisme, W., J. Li, T. Goldmann, S. Bolch, U. Wolfrum, and W.C. Smith. 2010. Light-dependent translocation of arrestin in rod photoreceptors is signaled through a phospholipase C cascade and requires ATP. *Cell. Signal.* 22:447–456. doi:10.1016/j.cellsig.2009.10.016

Ou, G., M. Koga, O.E. Blacque, T. Murayama, Y. Ohshima, J.C. Schafer, C. Li, B.K. Yoder, M.R. Leroux, and J.M. Scholey. 2007. Sensory ciliogenesis in *Caenorhabditis elegans*: assignment of IFT components into distinct modules based on transport and phenotypic profiles. *Mol. Biol. Cell.* 18:1554–1569. doi:10.1091/mbc.E06-09-0805

Papermaster, D.S. 2002. The birth and death of photoreceptors: the Friedenwald Lecture. *Invest. Ophthalmol. Vis. Sci.* 43:1300–1309.

Pazour, G.J., C.G. Wilkerson, and G.B. Witman. 1998. A dynein light chain is essential for the retrograde particle movement of intraflagellar transport (IFT). *J. Cell Biol.* 141:979–992. doi:10.1083/jcb.141.4.979

Pazour, G.J., B.L. Dickert, and G.B. Witman. 1999. The DHC1b (DHC2) isoform of cytoplasmic dynein is required for flagellar assembly. *J. Cell Biol.* 144:473–481. doi:10.1083/jcb.144.3.473

Pazour, G.J., S.A. Baker, J.A. Deane, D.G. Cole, B.L. Dickert, J.L. Rosenbaum, G.B. Witman, and J.C. Besharse. 2002. The intraflagellar transport protein, IFT88, is essential for vertebrate photoreceptor assembly and maintenance. *J. Cell Biol.* 157:103–113. doi:10.1083/jcb.200107108

Pedersen, L.B., and J.L. Rosenbaum. 2008. Intraflagellar transport (IFT) role in ciliary assembly, resorption and signalling. *Curr. Top. Dev. Biol.* 85:23–61. doi:10.1016/S0070-2153(08)00802-8

Peterson, J.J., W. Orisme, J. Fellows, J.H. McDowell, C.L. Shelamer, D.R. Dugger, and W.C. Smith. 2005. A role for cytoskeletal elements in the light-driven translocation of proteins in rod photoreceptors. *Invest. Ophthalmol. Vis. Sci.* 46:3988–3998. doi:10.1167/iovs.05-0567

Pigino, G., S. Geimer, S. Lanzavecchia, E. Paccagnini, F. Cantele, D.R. Diener, J.L. Rosenbaum, and P. Lupetti. 2009. Electron-tomographic analysis of intraflagellar transport particle trains in situ. *J. Cell Biol.* 187:135–148. doi:10.1083/jcb.200905103

Qin, H., D.R. Diener, S. Geimer, D.G. Cole, and J.L. Rosenbaum. 2004. Intraflagellar transport (IFT) cargo: IFT transports flagellar precursors to the tip and turnover products to the cell body. *J. Cell Biol.* 164:255–266. doi:10.1083/jcb.200308132

Qin, P., and R.G. Pourcho. 2001. Immunocytochemical localization of kainate-selective glutamate receptor subunits GluR5, GluR6, and GluR7 in the cat retina. *Brain Res.* 890:211–221. doi:10.1016/S0006-8993(00)03162-0

Reidel, B., T. Goldmann, A. Giessl, and U. Wolfrum. 2008. The translocation of signaling molecules in dark adapting mammalian rod photoreceptor cells is dependent on the cytoskeleton. *Cell Motil. Cytoskeleton*. 65:785–800. doi:10.1002/cm.20300

Roepman, R., and U. Wolfrum. 2007. Protein networks and complexes in photoreceptor cilia. *In* Subcellular Proteomics: From Cell Deconstruction to System Reconstruction. E. Bertrand and M. Faupel, editors. Springer, Dordrecht, Netherlands. 209–235.

Rosenbaum, J.L., and G.B. Witman. 2002. Intraflagellar transport. *Nat. Rev. Mol. Cell Biol.* 3:813–825. doi:10.1038/nrm952

Rosenbaum, J.L., D.G. Cole, and D.R. Diener. 1999. Intraflagellar transport: the eyes have it. *J. Cell Biol.* 144:385–388. doi:10.1083/jcb.144.3.385

Sedmak, T., E. Sehn, and U. Wolfrum. 2009. Immunoelectron microscopy of vesicle transport to the primary cilium of photoreceptor cells. In *Primary cilia*. Methods in Cell Biology, vol. 94, R.D. Sloboda, editor. Academic Press, London. 259–272.

Setou, M., T. Nakagawa, D.H. Seog, and N. Hirokawa. 2000. Kinesin superfamily motor protein KIF17 and mLin-10 in NMDA receptor-containing vesicle transport. *Science*. 288:1796–1802. doi:10.1126/science.288.5472.1796

Signor, D., K.P. Wedaman, J.T. Orozco, N.D. Dwyer, C.I. Bargmann, L.S. Rose, and J.M. Scholey. 1999a. Role of a class DHC1b dynein in retrograde transport of IFT motors and IFT raft particles along cilia, but not dendrites, in chemosensory neurons of living *Caenorhabditis elegans*. *J. Cell Biol.* 147:519–530. doi:10.1083/jcb.147.3.519

Signor, D., K.P. Wedaman, L.S. Rose, and J.M. Scholey. 1999b. Two heteromeric kinesin complexes in chemosensory neurons and sensory cilia of *Caenorhabditis elegans*. *Mol. Biol. Cell.* 10:345–360.

Sloboda, R.D. 2005. Intraflagellar transport and the flagellar tip complex. *J. Cell. Biochem.* 94:266–272. doi:10.1002/jcb.20323

Snow, J.J., G. Ou, A.L. Gunnarson, M.R. Walker, H.M. Zhou, I. Brust-Mascher, and J.M. Scholey. 2004. Two anterograde intraflagellar transport motors cooperate to build sensory cilia on C. elegans neurons. *Nat. Cell Biol.* 6:1109–1113. doi:10.1038/ncb1186

Sung, C.H., and A.W. Tai. 2000. Rhodopsin trafficking and its role in retinal dystrophies. *Int. Rev. Cytol.* 195:215–267. doi:10.1016/S0074-7696 (08)62706-0

Tai, A.W., J.Z. Chuang, C. Bode, U. Wolfrum, and C.H. Sung. 1999. Rhodopsin's carboxy-terminal cytoplasmic tail acts as a membrane receptor for cytoplasmic dynein by binding to the dynein light chain Tctex-1. *Cell*. 97:877–887. doi:10.1016/S0092-8674(00)80800-4

tom Dieck, S., W.D. Altrock, M.M. Kessels, B. Qualmann, H. Regus, D. Brauner, A. Fejtová, O. Bracko, E.D. Gundelfinger, and J.H. Brandstätter. 2005.

Molecular dissection of the photoreceptor ribbon synapse: physical interaction of Bassoon and RIBEYE is essential for the assembly of the ribbon complex. *J. Cell Biol.* 168:825–836. doi:10.1083/jcb.200408157

Trojan, P., N. Krauss, H.W. Choe, A. Giessl, A. Pulvermüller, and U. Wolfrum. 2008. Centrins in retinal photoreceptor cells: regulators in the connecting cilium. *Prog. Retin. Eye Res.* 27:237–259. doi:10.1016/j.preteyeres.2008.01.003

Tsujikawa, M., and J. Malicki. 2004. Intraflagellar transport genes are essential for differentiation and survival of vertebrate sensory neurons. *Neuron*. 42:703–716. doi:10.1016/S0896-6273(04)00268-5

Usukura, J., and S. Obata. 1995. Morphogenesis of photoreceptor outer segments in retinal development. *Prog. Retin. Eye Res.* 15:113–125. doi:10.1016/1350-9462(95)00006-2

Wang, Q., J. Pan, and W.J. Snell. 2006. Intraflagellar transport particles participate directly in cilium-generated signaling in *Chlamydomonas*. *Cell*. 125:549–562. doi:10.1016/j.cell.2006.02.044

Wolfrum, U. 1991. Tropomyosin is co-localized with the actin filaments of the scolopale in insect sensilla. *Cell Tissue Res.* 265:11–17. doi:10.1007/BF00318134

Yau, K.W., and R.C. Hardie. 2009. Phototransduction motifs and variations. *Cell*. 139:246–264. doi:10.1016/j.cell.2009.09.029

Young, R.W. 1976. Visual cells and the concept of renewal. *Invest. Ophthalmol. Vis. Sci.* 15:700–725.